

# Encapsulation and Controlled Release of Heparin from Electrospun Poly(L-Lactide-co- $\epsilon$ -Caprolactone) Nanofibers

Yan Su<sup>a,b,c</sup>, Xiaoqiang Li<sup>a,b,c</sup>, Yinan Liu<sup>a,b,c</sup>, Qianqian Su<sup>d</sup>,  
Marcus Lim Wei Qiang<sup>e</sup> and Xiumei Mo<sup>a,b,c,\*</sup>

<sup>a</sup> State Key Laboratory for Modification of Chemical Fibers and Polymer Materials,  
Donghua University, Shanghai 201620, P. R. China

<sup>b</sup> Key Laboratory of Textile Science & Technology, Ministry of Education, Donghua University,  
Shanghai 201620, P. R. China

<sup>c</sup> Biomaterials and Tissue Engineering Laboratory, College of Chemistry & Chemical Engineering  
and Biotechnology, Donghua University, Shanghai 201620, P. R. China

<sup>d</sup> Department of Chemistry, National University of Singapore, 117543, Singapore

<sup>e</sup> Faculty of Engineering, Department of Mechanical Engineering,  
National University of Singapore, 117543, Singapore

Received 27 September 2009; accepted 15 November 2009

---

## Abstract

Poly(L-lactide-co- $\epsilon$ -caprolactone) nanofibers with heparin incorporated were successfully fabricated by coaxial electrospinning. The morphologies of electrospun nanofibers were studied by scanning electron microscopy (SEM), and a significant decrease in fiber diameter was observed with increasing heparin concentration. The transmission electron microscopy (TEM) images indicated that coaxial electrospinning could generate core-shell structure nanofibers which have the potential to encapsulate drugs (heparin in this study) into the core part of nanofibers. Approximately 80% of the encapsulated heparin was sustainedly and stably released from the fibrous composite in 14 days by a diffusion/erosion coupled mechanism. The release behavior of heparin from blend electrospun nanofibers was also studied and showed an obvious burst release in the initial stage. An *in vitro* proliferation test was conducted to study the effect of heparin released from nanofibers, and the results suggest that the heparin maintains its bioactivity after encapsulating with and delivery through coaxially electrospun fibers.

© Koninklijke Brill NV, Leiden, 2011

## Keywords

Coaxial electrospinning, controlled release, heparin, PLLACL

---

\* To whom correspondence should be addressed. E-mail: xmm@dhu.edu.cn

## 1. Introduction

Electrospinning is a simple and versatile method to prepare ultrathin fibers from polymer solutions or melts. The obtained fibers usually have a diameter from several nanometers to a few micrometers, mostly hundreds of nanometers [1–3]. Because of their small diameters, electrospun polymer nanofibers possess concomitant large specific surface areas which are propitious to adhesion and proliferation of human cells [4]. Additionally, non-woven fabrics (mats) made of electrospun polymer nanofibers offer a unique capability to control the pore sizes among nanofibers. The top-down nano-manufacturing process could produce continuous and low-cost nanofibers which are relatively easy aligned, assembled and processed into various applications. Many synthetic and/or natural polymers including, but not limited to, polylactide (PLA) [5], poly( $\epsilon$ -caprolactone) (PCL) [6], poly(glycolic-acid) (PGA) [7], poly(L-lactide-co- $\epsilon$ -caprolactone) (PLLACL) [8], proteins (e.g., collagen) [9] and polysaccharides (e.g., chitosan) [10] have been electrospun into nanofibrous mats as tissue-engineering scaffolds for a growing number of animal cells. Furthermore, polymer nanofibers obtained through electrospinning have been conducted for the application of drug release systems. Because of outstanding features such as extremely high surface area to volume ratio [5, 11, 12], electrospun nanofibers have several advantages over other dosage forms, including the drug-release profile, which can be finely tailored by a modulation on the morphology, porosity and composition of the nanofibers' membrane [13]; the very small diameter of the nanofibers can provide short diffusion passage length; and the high surface area is helpful to a mass transfer and efficient drug release.

For use as drug-delivery systems, there is particular interest in producing biodegradable nanofibers which could encapsulate and sustain releasing drugs or bio-growth factors for a long time [14]. The drug-release characteristics depend on how well the drug is encapsulated inside the resulting nanofibers. Low efficiency of drug delivery and burst release are some of the most difficult problems. Therefore, core-shell structure nanofibers were developed to overcome the burst release problem. In Huang's work, it was found that drugs such as gentamycin sulfate (GS) and Resveratrol (RT) were released smoothly at the very beginning of initial stage from nanofibers with core-shell structure [15]. Moreover, the core-shell type nanofibers could protect an unstable biological agent from aggressive environments, deliver the bioactive molecules or drugs in a sustained way, and functionalize the surface of nanostructures without affecting the core material. There are several methods to fabricate core-shell fibers with hydrophilic drugs incorporated including emulsion and coaxial electrospinning [16, 17]. However, the water-in-oil-type emulsion conducted in electrospinning leads to reduced loading efficiency, phase separation and increased drugs presence on the surface of fibers rather than uniformly inside the fibers [18]. Therefore, the most feasible and effective technique for producing core-shell nanofibers is coaxial electrospinning.

The changes occurring after a vein graft procedure, such as endothelial denudation, platelet adherence and leukocyte infiltration [19] can lead to the proliferation

of vascular smooth muscle cells (VSMCs) in the vessel media and the subsequent migration of these cells into the intima causing arterial stenosis. In the normal blood vessel, it has been found that heparan sulfate glycosaminoglycans present in the vessel wall help maintain VSMCs in a contractile, non-proliferative state [20]. However, after injury, the normal biochemical balance is disrupted leading to the myoproliferative response.

It is well known that heparin has long been known to inhibit the proliferation of VSMCs [21]. There are several modes of action for the anti-proliferative effect of heparin, including inhibition of immediate-early genes [22], inhibition of production of matrix-degrading proteases important for cell migration and proliferation [23] and inhibition of mitogen-activated protein kinase [24]. The controlled release of heparin to the site of vascular injury could be used to prevent the myoproliferative response as well as avoiding the associated problems of systemic drug delivery [25]. Application of anti-proliferative agents to the localized adventitial surface of injured blood vessels has been previously shown to be effective in reducing stenosis. Therefore, heparin incorporated into electrospun fibers provides a utilized option for the prevention of VSMCs proliferation around vascular grafts.

In the present study, core–shell structure nanofibrous mats with heparin incorporated in the core part were generated by coaxial electrospinning. PLLACL was selected to form the shell of nanofibers, because of its good biocompatibilities with both smooth muscle cells (SMCs) and endothelial cells (ECs) [4]. Furthermore, the biodegradation rate of PLLACL could be adjusted by changing the molar ratios of PLLA in the co-polymer. The morphologies of the fabricated nanofibrous mats were examined by scanning electron microscopy (SEM) and the core–shell structure was verified by transmission electron microscopy (TEM). Mechanical properties of the core–shell type and pure PLLACL nanofibrous mats were measured by a materials testing machine. The release behavior and kinetics of heparin from core–shell nanofibers was measured. The effectiveness of released heparin was investigated by testing their prevention of VSMCs proliferation.

## 2. Materials and Methods

### 2.1. Materials

PLLACL (130 kDa), 50% L-lactide, was purchased from Sigma-Aldrich (USA). 2,2,2-Trifluoroethanol (TFE) was purchased from Shanghai Fine Chemicals (P. R. China). Heparin (MW 13 kDa) was purchased from Runjie Medicine Chemical (P. R. China). All of the materials were used without any further purification. VSMCs were purchased from Institute of Biochemistry and Cell Biology of the Chinese Academy of Sciences (P. R. China).

### 2.2. Electrospinning

The core solution was obtained by adding 0.03, 0.06 and 0.12 g heparin in 10 ml distilled water, and the shell solution by resolving 0.6 g PLLACL in 10 ml TFE.

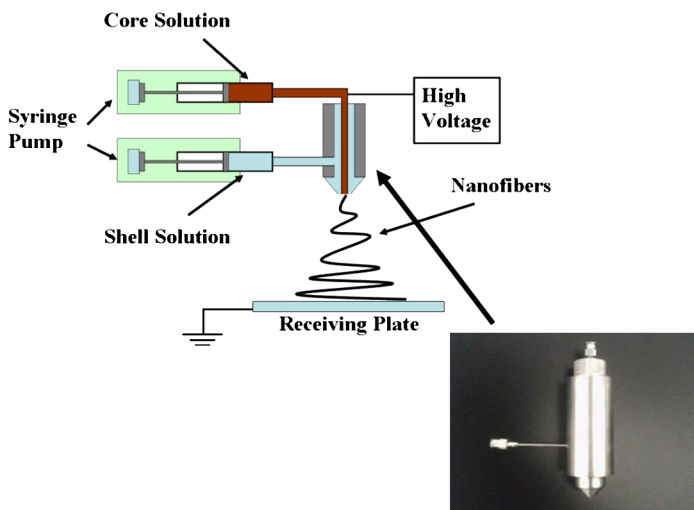


**Figure 1.** Basic setup for coaxial electrospinning, Inset: the special apparatus used in coaxial electrospinning. This figure is published in colour in the online edition of this journal, that can be accessed via <http://www.brill.nl/jbs>

The setup equipment briefly consisted of a syringe-like apparatus with an inner needle coaxially placed inside an outer one, as shown in Fig. 1. Two syringe pumps (Cole-Parmer, USA) were used to push the solutions from the inner and outer needles, respectively. The inner needle has an outer diameter of 1.0 mm; the outer needle has an inner diameter of 1.8 mm. A copper electrode was connected to the inner needle directly with a high voltage, which means that electrostatic potential was applied to the inner solution only. The electrical potential was transferred to the shell solution through the stainless steel co-axial needles depending on the conductivity of both the core and the shell solutions. An aluminum foil was grounded to collect ultrafine core-shell structure nanofibers. With an increase in the supplied voltage to a threshold value, a steady coaxial compound fluid jet was formed and ejected out of the tips of the syringe-like apparatus. The fluid jet was then thinned to a sub-micrometer size, after evaporation of the solvents during the course of jet flying to the foil; the thin jet was deposited on the collecting screen, forming the coaxial fibers. In our experiment, the inner and outer needle were connected through Teflon tubs to syringe pumps respectively, using which the core solution was injected at controlled flow rates of 0.1 ml/h, and the outer one was 1.0 ml/h. The distance between the needles and the collector was set at 12 cm. All of the electrospun nanofibers were obtained at an ambient temperature of 22–25°C with a relative humidity of 40–60%.

### 2.3. Fiber Morphology and Structure

The morphology of nanofibers was observed using a digital vacuum scanning electron microscope (JSM-5600LV, Jeol, Japan) at an accelerating voltage of 15 kV.

Samples for SEM observations were sputter-coated with gold prior to observation. The diameter of the electrospun ultrafine nanofibers was measured with image visualization software Image-J 1.34 (NIH, USA). Average fiber diameter and diameter distribution were determined by measuring about 60 random fibers from the SEM images.

Verification of the core–shell structure was conducted by TEM (H-800, Hitachi) at 100 kV, and the samples for TEM observations were prepared by collecting the nanofibers onto carbon-coated Cu grids.

#### 2.4. Mechanical Properties

Mechanical measurements were achieved by applying tensile test loads to specimens prepared from the co-axial electrospun nanofibers mats at the concentration and fluid flow rate mentioned previously. In this study, three specimens were prepared according to the method described by Huang *et al.* [26]. First, a white paper template was cut into templates of width  $\times$  length = 10 mm  $\times$  50 mm, and double-sided tape was glued onto the top and bottom areas of one side. The template was then glued onto the topside of the fiber mat and was cut into rectangular pieces along the vertical lines. After the aluminum foil was carefully peeled off, single sided tapes were applied onto the gripping areas as end-tabs. The resulting specimens had a planar dimension of width  $\times$  length = 10 mm  $\times$  30 mm. Mechanical properties were tested by a materials testing machine (H5K-S, UK) at 20°C, a relative humidity of 65% and an elongation speed of 10 mm/min. Three specimens were tensile tested to calculate the mean values and standard deviations for both pure PLLACL and coaxial electrospun PLLACL/heparin nanofiber mats.

#### 2.5. In Vitro Release Study

PLLACL nanofibrous mats loaded with different weight ratios of heparin were suspended in PBS (pH 7.4) solution in sealed 6-well plates. Three nanofibrous mats, each weighing  $100 \pm 5$  mg, were each soaked in 3.0 ml PBS (pH 7.4). Fibrous mats were incubated under static conditions at 37°C in the presence of 5% CO<sub>2</sub>. At various time points, 1.0 ml supernatant was retrieved from the wells and an equal volume of fresh medium was replaced. The concentration of each retrieved heparin solution was then determined by toluidine blue method. Toluidine blue (3.0 ml) was added into the supernatant which was retrieved from the wells and reacted adequately with heparin for 2 h at 37°C. Hexane (3.0 ml) was then added, and stirred vigorously to separate the heparin-toluidine blue complex formed. The aqueous solution of the samples was tested at 630 nm by an Agilent UV-Vis spectrophotometer (WFH-203B, PerkinElmer, USA).

#### 2.6. Vascular Smooth Muscle Cell Inhibition by Released Heparin

Either 50 mg 2 wt% heparin/PLLACL fibers, 100 mg 1 wt% heparin/PLLACL fibers, 200 mg 0.5 wt% heparin/PLLACL fibers, or 200 mg PLLACL fibers were sterilized with gamma rays and placed into 3 ml sterile cell culture media without fetal calf serum (FCS) and incubated at 37°C for 6 days. VSMCs plated at

$1 \times 10^4$  cells/cm<sup>2</sup> were allowed to attach overnight and then serum starved in 0.4% FCS media for 72 h to growth-arrest the cells. To stimulate proliferation, the media was supplemented with 5% FCS. Cells grown in 5% FCS media that had not been treated with fiber conditioned media were used as a positive control. To test the inhibitory effect of the heparin released from the fibers, the conditioned media from the 2, 1, 0.5 and 0 wt% heparin/PLLACL fibers was placed on the cells and FCS was added to a final concentration of 5%. The cells were then grown for 1, 3, 5 and 7 days under stimulation with FCS, with a media change conducted on day 3. After 1, 3, 5 and 7 days of seeding, VSMCs were quantified by the cell proliferation kit (C0009) purchased from the Beyotime Institute of Biotechnology (P. R. China) and an Enzyme-labeled Instrument (MK3) purchased from Thermo Fisher Scientific (USA) at 570 nm.

### 2.7. Morphology of Nanofibrous Mats after Release

Morphology of nanofibrous mats after drug release in PBS for 14 days was observed by Digital Vacuum Scanning Electron Microscope (JSM-5600LV, Jeol) at the accelerating voltage of 15 kV. Prior to SEM examination, the specimens were sputter-coated with gold to avoid charge accumulation.

### 2.8. Statistical Analysis

Statistical analysis was performed using Origin 7.5. Values (at least triplicate) were averaged and expressed as means  $\pm$  SD. Statistical differences were determined by one-Way ANOVA and differences were considered statistically significant at  $P < 0.05$ .

## 3. Results and Discussion

### 3.1. Fiber Morphology and Structure

In electrospinning, the traveling jet of polymer solution solidifies at the receiving plate with the evaporation of solvent(s) after exiting the needle and the solidified jet turns into nanofibers. PLLACL is easy to dissolve in many different solvents, such as acetone, chloroform and 1,1,1,3,3,3-hexafluoro-2-propanol. In this work, a water-soluble solvent (TFE) was used to prepare PLLACL solution. The effect of polymer concentration on fiber morphology had been studied at previous experiments with concentrations ranging from 0.02 to 0.16 g/ml. The results demonstrated that ultrafine PLLACL nanofibers with smooth surfaces could be electrospun at the concentrations between 0.04 and 0.12 g/ml. Furthermore, the fiber diameters increased with the increasing of polymer concentration. In this study, the coaxial electrospun polymer solution concentration was chosen at 0.06 g/ml.

The volatility of solvents is one of the most important factors in influencing the solidification process of electrospinning and also in influencing the morphologies of the electrospun nanofibrous mats. Because water has relatively low volatility, and may not be able to completely evaporate during electrospinning, it was found

that the presence of distilled water in the core solution could affect the formation of electrospun nanofibers.

In this study, PLLACL fibers were coaxially electrospun from 0.06 g/ml PLLACL in TFE solution and highly porous fiber mats could be formed without the occurrence of bead defects. The fibers appeared to be regular in shape and were deposited in a convoluted manner. Various parameters in the electrospinning process, such as polymer concentration, solution viscosity, electric field strength, feed rate of polymer solution and solution conductivity have been found to influence the fiber diameter. The conductivity of electrospinning solution can be altered by adding small molecules, such as ionic salts, which have electric charges. It was found that the presence of redundant charges in polymer solution leads to electrospun fibers with a substantially decreased diameter because the highly charged molecules in the spinning solution results in an increased charge density and this increased charge density causes greater elongation which makes the polymer jet into smaller diameter fibers. As shown in Fig. 2, with the increase of heparin (Na + salt) in the electrospun system fibers diameter decreased from  $765 \pm 98$  nm (nanofibers generated through pure PLLACL solution, Fig. 2a) to  $437 \pm 134$  nm (nanofibers produced by coaxial electrospinning with the inner solution of 0.012 g/ml heparin and outer solution of 0.06 g/ml PLLACL, Fig. 2d). Figure 3 shows the TEM micrographs of the core-shell structure of heparin/PLLACL nanofibers. The shell and the

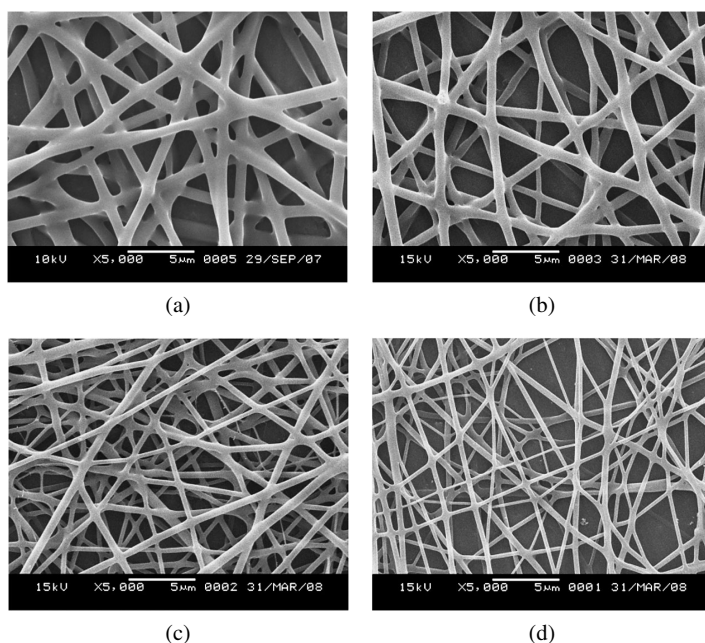


**Figure 2.** SEM images of the PLLACL/H nanofibers prepared from coaxial electrospinning contained different heparin amounts at (a) 0, (b) 0.5, (c) 1 and (d) 2 wt% PLLACL, and the amounts of heparin were controlled by concentrations of inner solutions.

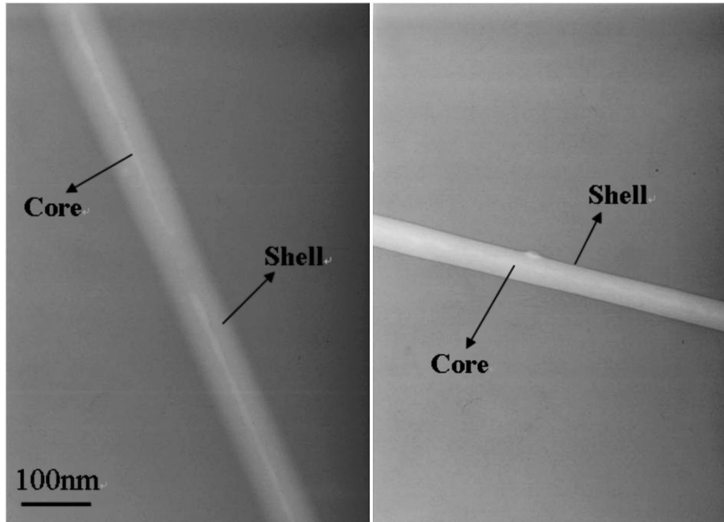


**Figure 3.** TEM micrographs of core-shell heparin/PLLACL nanofibers.

core in the images showing a clear interface indicated that heparin was encapsulated well into nanofibers.

### 3.2. Mechanical Properties of Coaxially Electrospun Nanofibrous Mats

One of the potential applications for coaxially electrospun nanofibers with heparin incorporated is to rehabilitate blood vessel rupture caused by traffic accidents or extreme mechanical forces. Therefore, mechanical properties of nanofibers are crucial for their success in tissue regeneration. In this study, nanofibrous mats were made by electrospinning of PLLACL-TFE solution and coaxial electrospinning with PLLACL-TFE as the shell solution, and heparin-distilled water as the core solution (0.012 g/ml). Representative tensile stress-strain curves of the electrospun nanofibrous mats are shown in Fig. 4. The average strength of PLLACL nanofibrous mats (Fig. 4b) was  $2.37 \pm 0.29$  MPa, which were higher than those of the coaxially electrospun nanofibrous mat (the average ultimate stress of three samples was  $1.88 \pm 0.24$  MPa). In our previous study, we had found the same phenomenon that incorporated bovine serum albumin (BSA) into nanofibers by coaxial electrospinning has negative effects on the mechanical properties of nanofibrous mats [17]. It is noted that heparin cannot conduct into fabricating nanofibers by electrospinning. Nonetheless, the matrix of the coaxially electrospun nanofibrous mat was PLLACL which was identical to that in the neat PLLACL nanofibrous mat; so that the ultimate strain of both nanofibrous mats were similar.

### 3.3. In Vitro Release Study

Heparin release profiles from coaxially electrospun PLLACL nanofibers with different heparin proportions are shown in Fig. 5a. Experiments were performed in

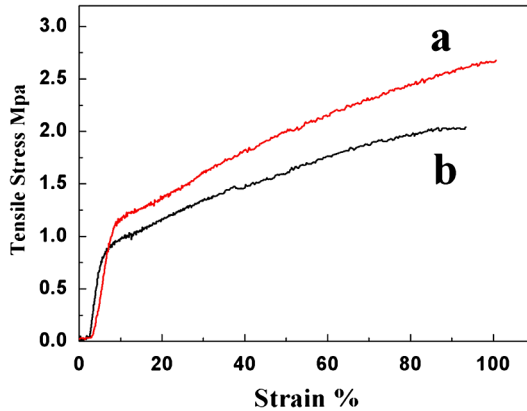


**Figure 4.** Representative tensile stress–strain curves of nanofibers mats. (a) PLLACL nanofibrous mat, (b) coaxial electrospun PLLACL/heparin nanofibrous mats (2 wt% heparin). This figure is published in colour in the online edition of this journal, that can be accessed *via* <http://www.brill.nl/jbs>

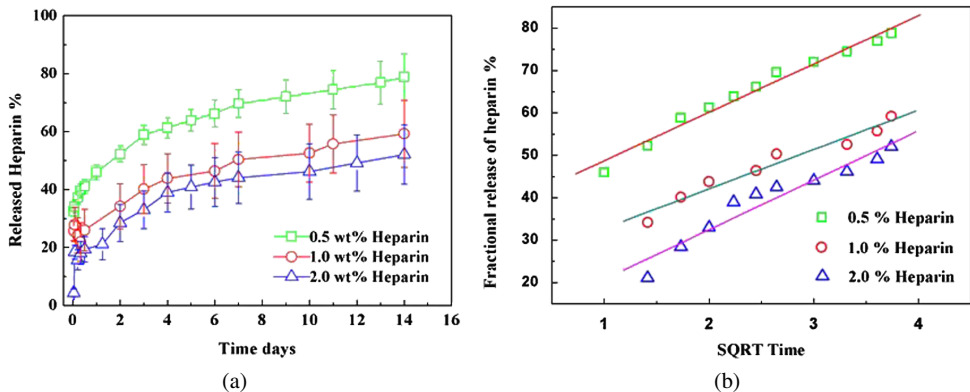


**Figure 5.** (a) *In vitro* heparin release profiles from PLLACL nanofibers which were fabricated by coaxial electrospinning with different heparin proportions. (b) Fractional release of heparin plotted as a function of the square root of time for 0.5, 1.0 and 2.0 wt% heparin encapsulated PLLACL fibers. This figure is published in colour in the online edition of this journal, that can be accessed *via* <http://www.brill.nl/jbs>

triplicate and error bars indicate standard deviation. The release processes for electrospinning cases can be illustrated by two stages: an initial fast release (stage I) followed by a constant release (stage II). In stage I, there were initial burst releases from electrospun mats, and the amount was 20–45%. The burst release of heparin from the fibers may be beneficial in preventing the myoproliferative response as heparin treatment begun immediately at the time of injury is more effective than a delayed administration. After the initial burst release, the release curves exhibited the sustained behavior. The whole release process went on for 14 days, until the total amount released was about 70%. This shows that the release was not complete, and the rest of them may release for a longer time.

In an attempt to analyze the release mechanism in greater detail, the coaxially electrospun fibrous mat system was modeled as a polydispersion of cylinders. The transport mechanism was compared with an ideal case of a monodispersion of cylinders. Therefore, the fractional amount of heparin released was plotted against the square root of time. The linear relationship (Fig. 5b) suggests Fickian diffusional release of the drug from the polymer, with the slope being proportional to the diffusion coefficient. The Fickian plot for the 0.5 wt% heparin/PLLACL fibers was linear ( $R = 0.98844$ ), as was the plot for the 1.0 wt% heparin/PLLACL fibers ( $R = 0.97897$ ) and for the 2.0 wt% heparin/PLLACL fibers ( $R = 0.96355$ ) from 1 to 14 days (Fig. 5b). In this study, we found that the relative rate of heparin release was faster when the nanofibrous mat was loaded with less heparin. A similar observation was reported by Huang *et al.* [27]. The heparin release rate could be adjusted by the ratio of the thickness of the shell to that of the core. From the release profile, the heparin release mechanism seemed to be *via* diffusion and erosion coupled mechanism. From Fig. 6, the morphology of nanofibrous mats was changed after release; however, the degradation degree was not high, indicating that heparin is released from fibrous mats by a diffusion/erosion coupled mechanism; however, diffusion through the pores of fibers may be the main pathway.

### 3.4. Morphology of Nanofibrous Mats after Release

In this study, the degradability and morphological sustainability of the electrospun composite nanofibrous mats were also investigated after immersion in PBS for 14 days. Degradation profiles of the electrospun fibrous mats were evaluated by

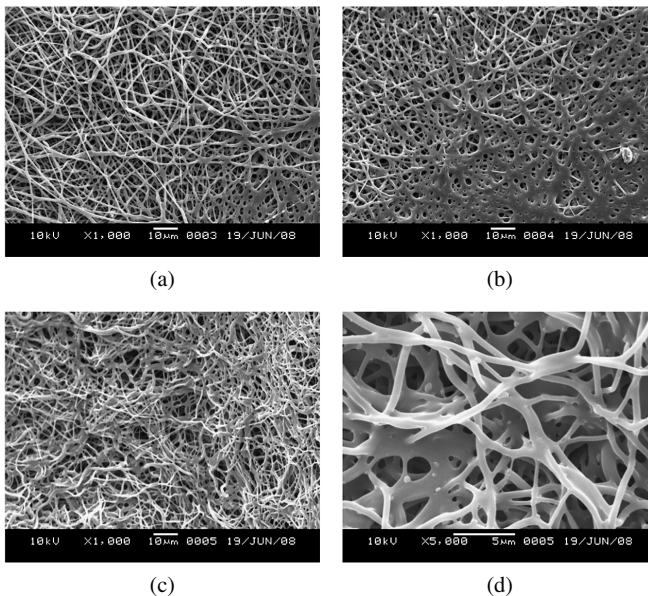


**Figure 6.** SEM images showing representative morphologies of the nanofibrous mats after 14 days release. (a) 0.5%, (b) 1.0%, (c, d) 2.0% heparin in nanofibers.

SEM and shown in Fig. 6. In contrast to the smooth surface of fibers before incubation (shown in Fig. 1), visible changes of fibers morphologies were observed on SEM images. The electrospun fibers with 0.5% heparin incorporated almost retained their original morphology (fiber diameter was larger) after incubation in PBS for 336 h. By contrast, nanofibrous mats with 1.0 and 2.0% heparin incorporated have clearly lost their original morphologies after immersing in PBS (Fig. 6b–d). From Fig. 2, it can be seen that more heparin was contained; the diameter of the nanofibers was smaller. Also, small diameter fibers enhanced the specific surface areas. Furthermore, there are more heparin released from the nanofibers membrane incorporated more heparin. All of these may result in higher degree of degradation of nanofibrous mats with more heparin.

### 3.5. In Vitro Bioactivity Study

To evaluate the bioactivity of released heparin, their capability to inhibit the proliferation of VSMCs was tested. VSMCs were seeded and cultivated on the neat PLLACL nanofibrous mats, PLLACL/heparin nanofibrous mats (with heparin of 0.5, 1.0 and 2.0%), as well as the standard tissue culture plates (TCPs, which were coated with collagen). The amount of VSMCs (reflected by MTT absorbency) increased with the increasing of culture time both on the PLLACL fibrous mats and TCPs as shown in Fig. 7. This result indicates that neither the degradation products from PLLACL fibers (if present) nor the morphology changes of PLLACL fibers has an inhibitory effect on cell growth. However, VSMCs present a bad proliferation on the fibrous mats with heparin incorporated compared with neat PLLACL and TCP because released heparin inhibited the growth. This demonstrates that he-

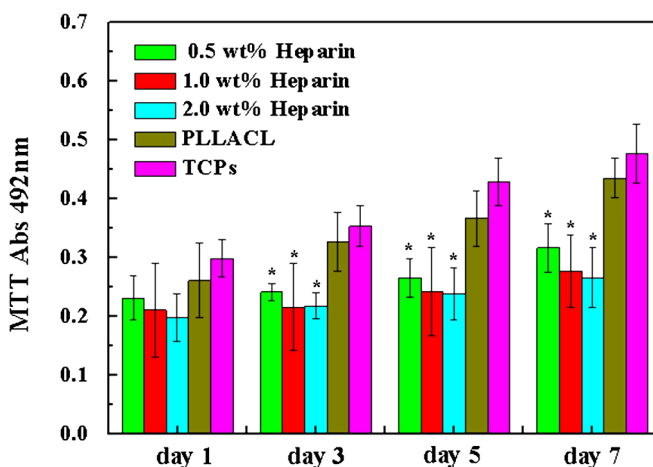


**Figure 7.** Proliferation of VSMCs cultured on the neat PLLACL nanofibrous mats, the PLLACL/Heparin (with 0.5, 1.0 and 2.0% heparin) nanofibrous mats, and the standard tissue-culture plates (TCPs) (mean  $\pm$  SD,  $n = 3$ ). Statistical difference between groups is indicated (\* $P < 0.05$ ). This figure is published in colour in the online edition of this journal, that can be accessed via <http://www.brill.nl/jbs>

parin retained its capability after encapsulation by coaxially electrospinning and the release from PLLACL fibers.

#### 4. Conclusion

The objective of this study was to investigate coaxially electrospun PLLACL nanofibrous mats with heparin incorporated. The coaxially electrospun nanofibrous mats from PLLACL could possess the unique combined characteristics of cell-growth scaffolds and controllable drug-releasing agents. In this study, PLLACL/heparin nanofibers were successfully prepared by coaxial electrospinning of PLLACL solution (as the shell solution) and heparin solution (as the core solution). The release study confirms that heparin encapsulated in nanofibers by coaxial electrospinning could be released stably and sustainedly. The bioactivity of heparin released from PLLACL nanofibers was investigated by the VSMCs inhibition study. The scaffold prepared by electrospinning PLLACL/heparin has potential in the application of blood vessel tissue engineering.

#### Acknowledgements

This research was supported by National science foundation (30570503), National high technology research and developed program (863 Program, 2008AA03Z305), Science and technology commission of Shanghai municipality program (08520704600 and 0852nm03400), and “111 Project” (B07024).

#### References

1. D. H. Reneker, A. L. Yarin, E. Zussman and H. Xu, *Adv. Appl. Mech.* **41**, 43 (2007).
2. T. J. Sill and H. A. von Recum, *Biomaterials* **29**, 1989 (2008).
3. Z. M. Huang, Y. Z. Zhang, S. Ramakrishna and C. T. Lim, *Polymer* **45**, 5361 (2004).
4. X. M. Mo, C. Y. Xu, M. Kotaki and S. Ramakrishna, *Biomaterials* **25**, 1883 (2004).
5. E. R. Kenawy, G. L. Bowlin, K. Mansfield, J. Layman, D. G. Simpson, E. H. Sanders and G. E. Wnek, *J. Control. Rel.* **81**, 57 (2002).
6. F. Chen, C. N. Lee and S. H. Teoh, *Mater. Sci. Eng. C* **27**, 325 (2007).
7. Y. You, S. W. Lee, J. H. Youk, B. M. Min, S. J. Lee and W. H. Park, *Polym. Degrad. Stabil.* **90**, 441 (2005).
8. F. Chen, X. Q. Li, X. M. Mo, C. L. He, H. S. Wang and Y. Ikada, *J. Biomater. Sci. Polymer Edn* **19**, 677 (2008).
9. J. A. Matthews, G. E. Wnek, D. G. Simpson and G. L. Bowlin, *Biomacromolecules* **3**, 232 (2002).
10. N. Bhattarai, D. Edmondson, O. Veiseh, F. A. Matsen and M. Q. Zhang, *Biomaterials* **26**, 6176 (2005).
11. Y. Su, X. Q. Li, L. J. Tan, C. Huang and X. M. Mo, *Polymer* **50**, 4212 (2009).
12. S. Y. Chew, J. Wen, K. F. Yim and K. W. Leong, *Biomacromolecules* **6**, 2017 (2005).
13. N. Ashammakhi, A. Ndreu, A. M. Piras, L. Nikkola, T. Sindelar and H. Ylikauppila, *J. Nanosci. Nanotechnol.* **7**, 862 (2007).
14. Z. M. Huang and A. H. Yang, *Acta Polym. Sin.* **1**, 48 (2006).

15. Z. M. Huang, C. L. He, A. Z. Yang, Y. Z. Zhang, X. J. Hang, J. L. Yin and Q. S. Wu, *J. Biomed. Mater. Res. A* **77**, 169 (2006).
16. Y. Yang, X. H. Li, M. B. Qia, S. B. Zhou and J. Weng, *Eur. J. Pharm. Biopharm.* **69**, 106 (2008).
17. X. Q. Li, Y. Su, R. Chen, C. L. He, H. S. Wang and X. M. Mo, *J. Appl. Polym. Sci.* **111**, 1564 (2009).
18. X. L. Xu, L. X. Yang, X. Y. Xu, X. Wang, X. S. Chen and Q. Z. Liang, *J. Control. Rel.* **108**, 33 (2005).
19. G. M. Hirsch and M. J. Karnovsky, *Am. J. Pathol.* **139**, 581 (1991).
20. J. J. Castellot, Jr., L. V. Favreau, M. J. Karnovsky and R. D. Rosenberg, *J. Biol. Chem.* **257**, 11256 (1982).
21. Z. H. Yang, P. Birkenhauer, F. Julmy, D. Chickering, J. P. Ranieri, H. P. Merkle, T. F. Luscher and B. Gander, *J. Control. Rel.* **60**, 269 (1999).
22. L. A. Pukac, J. J. Castellot, Jr., T. C. Wright, Jr., B. L. Caleb and M. J. Karnovsky, *Cell Regul.* **1**, 435 (1990).
23. R. D. Kenagy, S. T. Nikkari, H. G. Welgus and A. W. Clowes, *J. Clin. Invest.* **93**, 1987 (1994).
24. K. Mishra-Gorur and J. J. Castellot, Jr., *J. Cell. Physiol.* **178**, 205 (1999).
25. E. Luong-Van, L. Grøndahl, K. N. Chua, K. W. Leong, V. Nurcombe and S. M. Cool, *Biomaterials* **27**, 2042 (2006).
26. Z. M. Huang, Y. Z. Zhang, S. Ramakrishna and C. T. Lim, *Polymer* **45**, 5361 (2004).
27. H. H. Huang, C. L. He, H. S. Wang and X. M. Mo, *J. Biomed. Mater. Res. A* **90**, 1243 (2009).